ICA 2019 AACHEN

PROCEEDINGS of the
23rd International Congress on Acoustics

9 to 13 September 2019 in Aachen, Germany

Synthesis of the inerter by direct acceleration feedback

Neven ALUJEVIĆ[1]; Ivan ĆATIPOVIĆ[1]; Hinko WOLF[1]; Nikola VLADIMIR[1]

[1] University of Zagreb, Faculty of Mechanical Engineering and Naval Architecture, Croatia

ABSTRACT

Physical realisations of the inerter are often such that they must be either large scale, i.e. rack and pinion inerters, or they inherently include additional elements in parallel or in series with the inerter, i.e. shunted electromechanical transducers or active force feedback inerter realisations, or alternatively they bring along a large parasitic damping, i.e. fluid-based inerters. In this study inerter is realised by feeding back the subtracted outputs of two accelerometers attached to a reactive force actuator terminals. Although in theory such feedback loop is unconditionally stable due to the collocated sensor-actuator arrangement, in practice it may not exhibit good stability properties due to the lack of duality between the sensors and the actuator in conjunction with the internal dynamics of the transducers. Therefore in this paper dynamics of seismic accelerometer sensors and an electrodynamic actuator are fully incorporated into a theoretical model of such an inerter. The inerter model is coupled to a two degree of freedom mechanical system in order to study the stability of the feedback loop and the maximum possible synthesisable inertance. The results indicate that it is crucial to have a highly damped accelerometer resonance in order to achieve good stability and large synthesised inertance.

Keywords: Interter, Active vibration control, Vibration isolation

1. INTRODUCTION

Inerter is a one-port, two-terminal element in mechanical networks which resists *relative* acceleration across its two terminals. The coefficient of resistance, *the inertance,* is measured in kilograms. The inerter fills an empty niche enabling a complete analogy between mechanical and electrical networks, the electrical analogue of the inerter being the capacitor (1,2). In the framework of mechanical network analysis, it is typically assumed that the inerter behaves in an idealised way, i.e. that it can be represented through its inertance only. Such idealisations are ordinarily assumed for elements like springs, dampers, inductances or resistors in lumped parameter mechanical or electrical networks. However, a realistic element, for example a helical spring, can itself exhibit a rich dynamic behaviour (3). This is equally true for other elements of lumped parameter mechanical systems. Fidelity of single-parameter representations of physical mechanical network elements depends on how the element is designed in practice.

Mechanical inerter designs include rack and pinion inerters (4), ball-screw inerters (5), and helical fluid channel inerters (6). One of the most important characteristics of any physical realisation of the inerter is the ratio of its inertance to its mass. This ratio is normally required to be large so as to enhance inertia effects of lightweight structures without significantly increasing their mass. In mechanical inerter designs the inertance can be several hundred times larger than the mass of the inerter itself (4). However, such inerters are typically mid to large scale and are not suitable for vibration control purposes in small scale applications due to their large dimensions and large stroke. Furthermore, effects such as friction, stick-slip of the gear pairs, or the elasticity of the gears and connecting rods are inevitably present in gear-train inerter constructions. On the other hand, a relatively large parasitic non-linear damping characterises the fluid-based inerters (6).

Another class of inerter realisations are the electromechanical inerters. In these systems electomechanical transducers are shunted with appropriate electrical impedances at their electrical ports in order to generate inertance-like effects at their mechanical ports. Small scale

[1] neven.alujevic@fsb.hr

electromechanical transducers are characterised by a relatively low energy conversion efficiency (7), so it is necessary to use non-Foster shunt circuits in order to compensate for losses in the transducers (8). This makes the approach active, which on one hand requires energy and on the other a careful regard of the stability and robustness of the system. Nevertheless, it is possible to synthesise an ideal inerter element connected to additional elements that occur as a side-effect of using a particular shunting technique. For example, by shunting a voice coil transducer with a certain negative impedance electrical circuit, an inerter connected in series with a parallel spring damper-pair can be synthesised (8). The additional lumped parameter elements in the equivalent mechanical network may or may not be desirable.

Further active approaches to realise the inerter include the force feedback approach (9,10). Here a pair of collocated reactive actuators and a force sensor are used so as to feed back the output of the force sensor through both single and double integrators to drive the actuator. In such a way the inerter can be synthetized which is connected in series with a damper (10).

In this paper, an attempt is made to synthesise the inerter by direct acceleration feedback control system. Outputs of two accelerometers mounted at the two terminals of a force actuator are subtracted to form a relative acceleration error signal which is amplified through an adjustable gain and fed to the actuator. In this way it may be possible to realise a small-scale inerter with an actively tuneable inertance without additional elements in parallel or in series to the inerter. Classical inertial accelerometers and a small scale voice-coil actuator are assumed. Although the control approach is physically well-founded, its application is not straightforward. For example, the relative acceleration sensor is collocated to the reactive force actuator, but the two transducers are not dual (11,12), i.e. they are not complementary in terms of mechanical power. As a result, the inherent frequency response of the sensor-actuator transducers can inhibit the stability of the feedback loop, as discussed in reference (13), for example.

A fully coupled electromechanical model of a two degree of freedom mechanical system equipped with the described active control loop is formulated in this paper. The dynamics of the inertial accelerometers and the electrodynamic actuator are modelled in detail. The coupled model is used to study the stability of the feedback loop and to assess the range of synthesizable inertances that could be used to isolate simple harmonic discrete vibrations coming from a flexible base to sensitive equipment mounted on it. In the second section of the paper the model problem is described and the mathematical model is formulated. In the third section the stability and the response of the active system are discussed, which is followed by the conclusions section.

2. MODEL PROBLEM

The mechanical system considered is a lumped parameter two degree of freedom (DOF) system shown in Figure 1. This system is a representation of the vibration isolation problem in which the sensitive equipment, m_2, is suspended with a spring k_2 and a damper c_2 onto a flexible base characterized by the mas m_1, stiffness k_1 and a damper c_1. Dynamic excitation is applied to the base mass through the simple harmonic primary force f_p. The formulation presented in this paper considers time-harmonic functions, which are defined in complex form $f(t) = \mathrm{Re}\left\{ f(\omega) e^{\mathrm{i}\omega t} \right\}$, where $f(\omega)$ is the complex amplitude of the function ω is the circular frequency and $\mathrm{i} = \sqrt{-1}$. As normally done in vibration studies, the formulation that follows thus refers to the complex amplitudes $f(\omega)$ of the time-harmonic functions $f(t)$ and, for brevity, the frequency dependence is omitted.

As discussed in, for example, (14), with the inclusion of the inerter of inertance b_2 into the suspension, Figure 1 (b), a zero can be assigned to the transfer admittance between the primary force, f_p , and the displacement of the sensitive equipment, m_2, at the frequency $\omega_a = \sqrt{k_2 / b_2}$. If the damping coefficient c_2 is made low, this effectively creates an anti-resonance condition in the transfer admittance, so that the mass m_2 becomes unresponsive to simple harmonic forcing at $\omega = \omega_a$. Therefore a vibration isolation effect can be achieved provided that the inertance b_2 can be tuned so as to match the antiresonance frequency to the excitation frequency. If a small scale mechanical system is considered, then existing inerter designs probably cannot accomplish the task for reasons discussed in Introduction. Therefore it is reasonable to attempt to synthesise the inerter effects by using the feedback control loop shown schematically in Figure 1 (a). The purpose of the feedback loop is to

generate a control force proportional to the relative acceleration between the equipment and the base, that is, to emulate effects of the inerter, b_2, mounted in parallel to the suspension spring and damper, shown in Figure 1 (b).

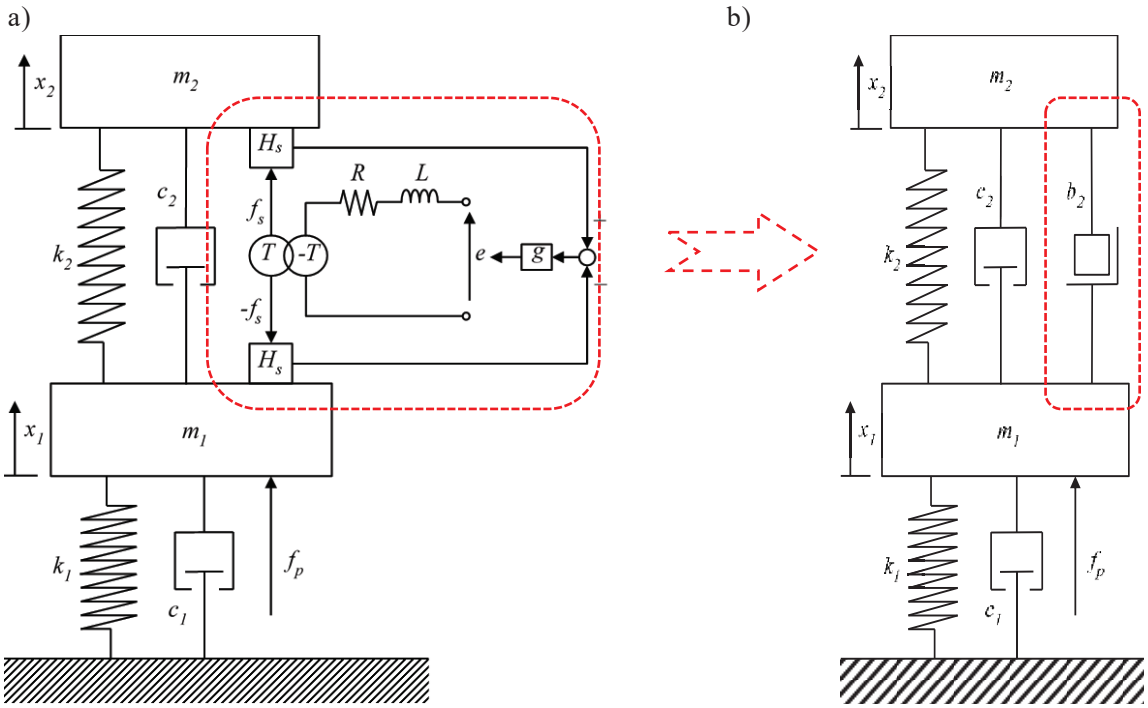

Figure 1: The 2 DOF mechanical system equipped with a direct acceleration feedback loop, plot (a), with the purpose of synthesizing the inerter, plot (b)

The control force, f_c, is applied by an electrodynamic actuator that reacts between the two masses. The actuator is characterized by a transducer coefficient T, which is often referred to as voice coil constant, inductance L, and the resistance R. The force generated by the actuator is proportional to the electrical current flowing through the transducer coil through the transducer coefficient T:

$$f_c = -Ti \tag{1}$$

The current i, however, depends both on the voltage applied at the transducer electrical terminals, e, and on the relative velocity, $s(x_2 - x_1)$, between its mechanical terminals, according to the following expression:

$$e = Ri + sLi + sT(x_2 - x_1) \tag{2}$$

where $s = \mathrm{i}\omega$.

In the present controller scheme the voltage, e, is made proportional to subtracted outputs of the two accelerometer sensors through a voltage amplifier gain, g, Figure 1 (a). The error signals are provided by two equal inertial accelerometers characterised by the transfer function H_s. This is the frequency response function (FRF) between the accelerometer output and the true acceleration of a structure onto which the accelerometer is attached. The two accelerometers are assumed to be much lighter than the sensitive equipment or the flexible base, so that their mechanical impedance can be entirely neglected. Therefore the voltage at the actuator electrical terminals is given by the control law:

$$e = gH_s s^2 (x_2 - x_1) \tag{3}$$

The dynamics of the mechanical parts of the system, i.e. the system without the control loop elements encircled by the red dashed line in Figure 1, can be represented by four mobility functions $Y_{i,j}$. They are the FRFs between the velocity of the mass i due to a force acting at the mass j. If i=j the corresponding mobility is referred to as driving point mobility, otherwise it is referred to as a transfer mobility. By considering contributions of the primary and the control forces one can write:

$$sx_1 = Y_{1,1} f_p - Y_{1,1} f_c + Y_{1,2} f_c \tag{4}$$

$$sx_2 = Y_{2,1}f_p - Y_{2,1}f_c + Y_{2,2}f_c \tag{5}$$

By taking into account Eqs. (1-5) and the reciprocity principle that imposes $Y_{2,1} = Y_{1,2}$, the fully coupled closed loop response of the system can be calculated in terms of five FRFs:

$$H_{e,f_p} = \frac{sgH_s\left(Y_{1,2} - Y_{1,1}\right)\left(R + Ls\right)}{D_1} \tag{6}$$

$$H_{i,f_p} = \frac{\left(Y_{1,1} - Y_{1,2}\right)\left(T - sgH_s\right)}{D_1} \tag{7}$$

$$H_{f_c,f_p} = -TH_{i,f_p} \tag{8}$$

$$H_{x_1,f_p} = \frac{\left(Y_{1,2}{}^2 - Y_{1,1}Y_{2,2}\right)T^2 + sgH_s\left(Y_{1,1}Y_{2,2} - Y_{1,2}{}^2\right)T + Y_{1,1}\left(R + Ls\right)}{D_1 s} \tag{9}$$

$$H_{x_2,f_p} = \frac{\left(Y_{1,2}{}^2 - Y_{1,1}Y_{2,2}\right)T^2 + sH_s\left(Y_{1,1}Y_{2,2} - Y_{1,2}{}^2\right)T + Y_{1,2}\left(R + Ls\right)}{D_1 s} \tag{10}$$

where $D_1 = \left(2Y_{1,2} - Y_{1,1} - Y_{2,2}\right)T^2 + gH_s\left(Y_{1,1} - 2Y_{1,2} + Y_{2,2}\right)sT + R + Ls$, H_{e,f_p} is the FRF between the actuator voltage and the primary excitation force, H_{i,f_p} is the FRF between the actuator current and the primary excitation force, H_{f_c,f_p} is the FRF between the control force and the primary excitation force, H_{x_1,f_p} is the closed loop driving point receptance, and H_{x_2,f_p} is the closed loop transfer receptance.

The sensor-actuator open loop frequency response function can be obtained by calculating the FRF between the subtracted accelerometer outputs and the voltage fed to the actuator in absence of the primary excitation:

$$H_{s,a} = s^2 H_s\left(x_2 - x_1\right)\Big|_{f_p = 0} \tag{11}$$

This can be done by substituting $f_p = 0$ into Eqs. (4,5) and taking into account also Eqs. (1-3):

$$H_{s,a} = \frac{sH_sT\left(2Y_{1,2} - Y_{2,2} - Y_{1,1}\right)}{\left(2Y_{1,2} - Y_{2,2} - Y_{1,1}\right)T^2 + R + Ls} \tag{12}$$

The transfer function H_s characterising the two accelerometer sensors can be written as (15):

$$H_s = \frac{\omega_A{}^2}{\omega_A{}^2 + 2\zeta_A\omega_A s + s^2} \tag{13}$$

where ω_A is the mounted natural frequency of the accelerometer, and ζ_A is the accelerometer damping ratio. For simplicity, it is assumed that the accelerometer sensitivity is absorbed in the feedback gain *g*. In other words, the accelerometer transfer function has been normalised so as to have a unit sensitivity for static accelerations.

The four mechanical mobility functions $Y_{i,j}$ are, (14):

$$Y_{1,1} = \frac{s\left(s^2 m_2 + sc_2 + k_2\right)}{D_2} \tag{14}$$

$$Y_{2,1} = Y_{1,2} = \frac{s\left(sc_2 + k_2\right)}{D_2} \tag{15}$$

$$Y_{2,2}\frac{s\left(s^2 m_1 + \left(c_1 + c_2\right)s + k_1 + k_2\right)}{D_2} \tag{16}$$

where $D_2 = s^4 m_1 m_2 + \left(\left(c_1 + c_2\right)m_2 + m_1 c_2\right)s^3 + \left(\left(k_1 + k_2\right)m_2 + m_1 k_2 + c_1 c_2\right)s^2 + \left(k_1 c_2 + c_1 k_2\right)s + k_1 k_2$.

3. DISCUSSION

In order to assess the stability of the feedback loop, Nyquist criterion is used. The sensor-actuator open-loop FRF, Eq. (12), is plotted using Bode and Nyquist diagrams for an example small scale vibration isolation model problem. The properties of the system are given in Table 1.

Table 1 – Properties of the example system

Parameter	Value
m_1 (kg)	0.1
m_2 (kg)	0.05
k_1 (N/m)	1000
k_2 (N/m)	500
c_1 (Ns/m)	1
c_2 (Ns/m)	1
T (N/A,Vs/m)	0.45
L ($\cdot 10^6$ H)	63
R (Ω)	1.5

The properties of the actuator correspond to an off-the-shelf miniature moving coil linear motor (16). The properties of the two accelerometers are varied in order to illustrate their influence on the stability of the control loop. A situation if first considered assuming a standard, general purpose piezoelectric accelerometer whose natural frequency and damping ratio have been identified by matching the sensitivity function, H_s, Eq. (13), with that from its datasheet (17). The match can be seen in Figure 2, and the identified values of the mounted natural frequency and the damping ratio are: $f_A = 2\pi\omega_A = 42$ kHz and $\zeta_A = 0.0158$. The agreement between the model results and the measured data is very good so the simple accelerometer model given by Eq. (13) is valid.

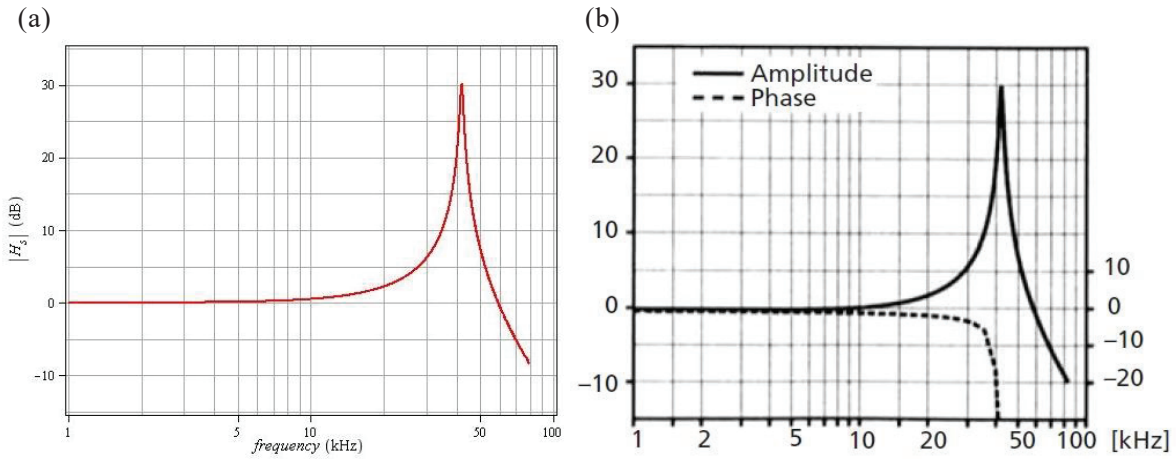

Figure 2: The transfer function, H_s, of the two accelerometer sensors, plot (a): model, plot (b): measured

However, the stability analysis indicates that such an accelerometer is not appropriate for the task considered in this study. As shown by Bode plot of the open loop sensor-actuator FRF in Figure 3 (a), the combination of the gradual phase lag of 45 degrees due to the inductance of the actuator coil and the abrupt 180 degree phase lag due to the second order accelerometer dynamics, causes the locus of the FRF to cross the negative real axis in the Nyquist plot, shown in Figure 3 (b). Furthermore, the amplitude at the crossover frequency of 42 kHz (the accelerometer mounted resonance frequency) is very large due to the low accelerometer damping ζ_A. The amplitudes of the sensor-actuator open-loop FRF at the two resonances due to the mechanical system response are in fact significantly lower

that that due to the accelerometer resonance. As a result, no significant gain can be implemented assuming standard gain margins and no significant inertance can be synthesised.

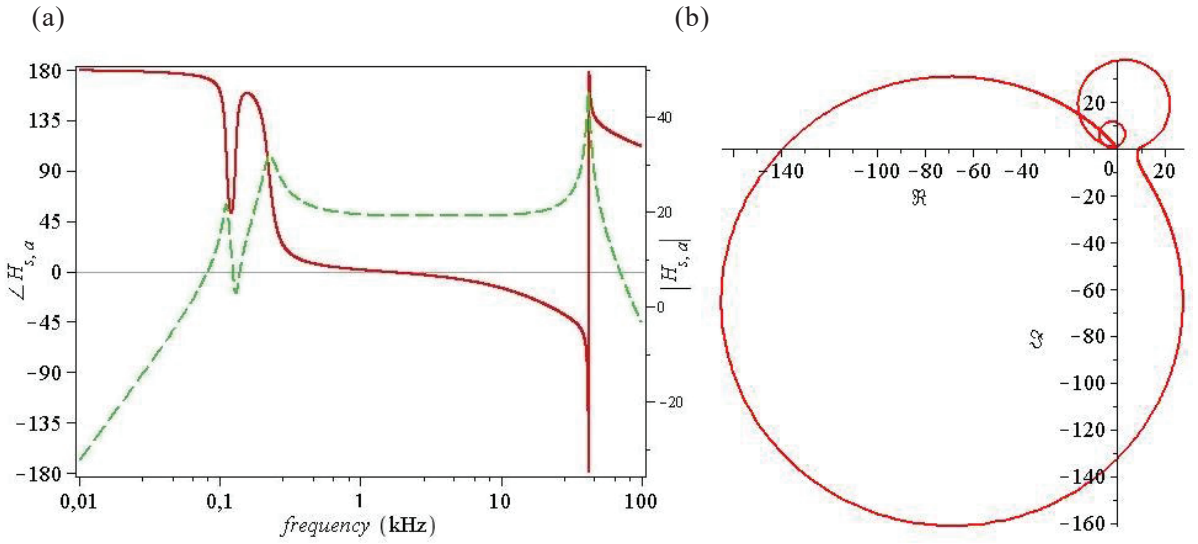

Figure 3: (a) Bode and (b) Nyquist plots of the open loop sensor-actuator FRF, $H_{s,a}$, with $f_A = 42$ kHz and $\zeta_A = 0.0158$.

A situation in which the accelerometer damping ratio is increased to its critical value $\zeta_A = 1$ with unchanged mounted resonance frequency is considered next. In this case the feedback gain can be set to g= 0.43 V/V with a gain margin of 6 dB, as can be seen in the zoomed area of plot (b) of Figure 4, since the locus crosses the negative real axis with the amplitude of 0.5. (The open loop sensor – actuator FRF has been multiplied by the feedback gain).

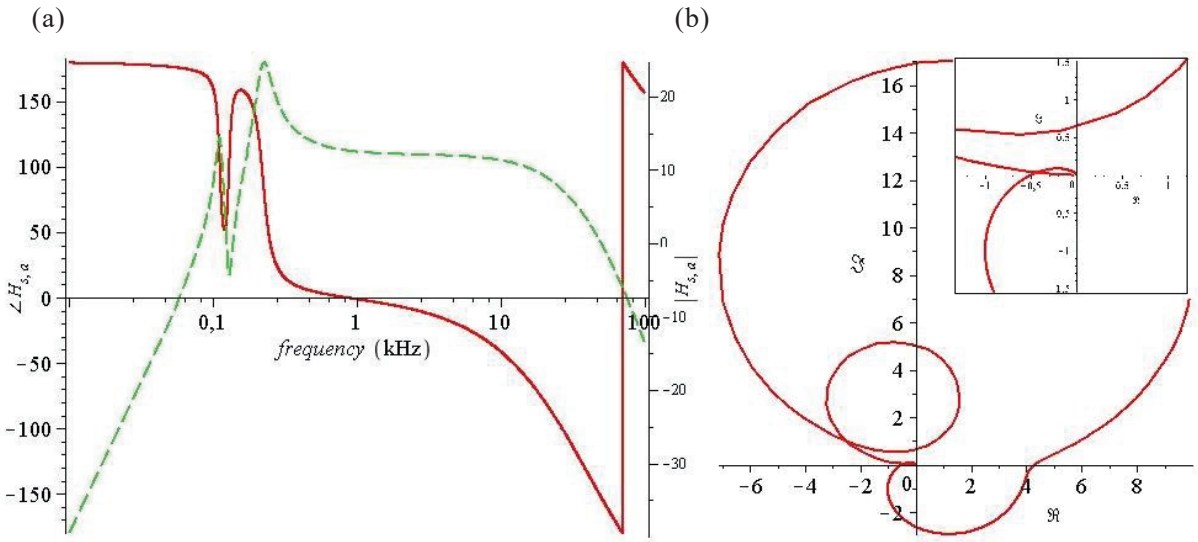

Figure 4: (a) Bode and (b) Nyquist plots of the open loop sensor-actuator FRF, $H_{s,a}$, with $f_A = 42$ kHz and $\zeta_A = 1$, assuming the feedback gain of g= 0.43 *V/V*

This control loop synthesises the desired inertance, which can be seen in Figure 5, red solid line. In fact, the figure shows the amplitude of the transfer receptance H_{x_2,f_p} for four cases. The first case is with the open loop system. In this case there can be seen two resonances due to the mechanical degrees of freedom and no antiresonances, as one might expect for transfer admittances in a 2 DOF mechanical systems. However, if the feedback loop is closed with g= 0.43 V/V, ensuring a gain margin

of 6 dB, then an antiresonance appears at the frequency of approximately 100 Hz. This corresponds to a synthetized inertance of $b_2 = k_2 / \omega_A^2 = 500/(2\pi \cdot 100)^2$ kg $= 0.0012$ kg. Therefore, at the frequency of 100 Hz the mass m_2 becomes rather unresponsive to the primary force f_p exciting the mass m_1 so that the desired isolation effect is achieved.

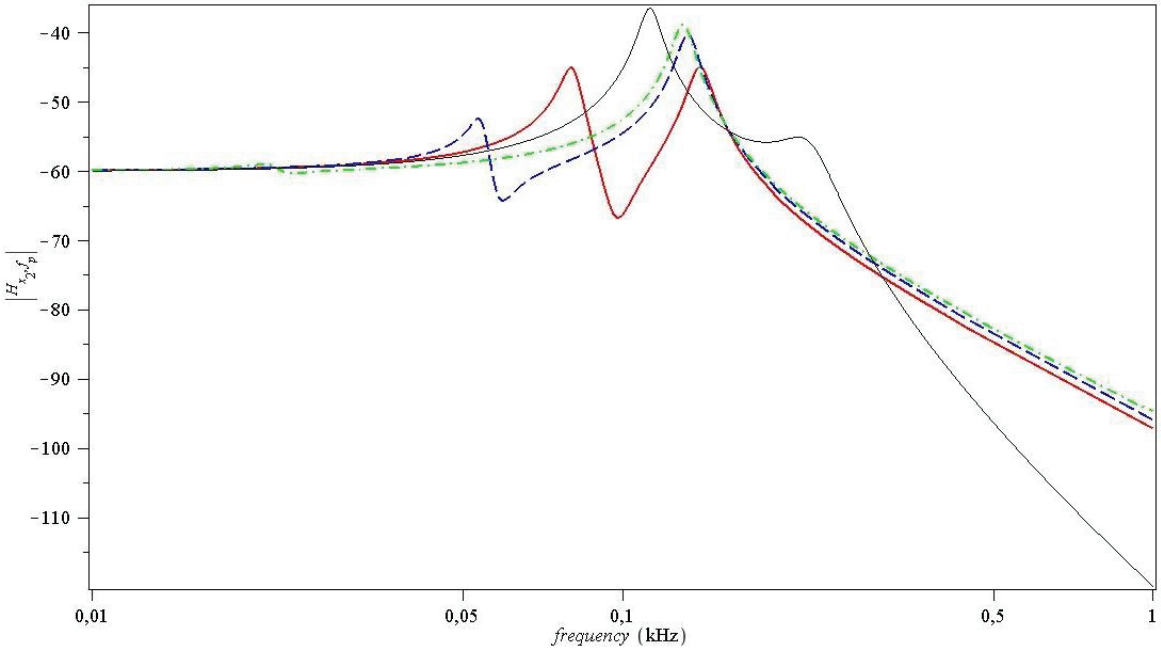

Figure 5: The closed loop transfer receptance, H_{x_2,f_p}, with no control (black faint line), and with control using the feedback gains of 0.43 (red solid line), 0.45 (blue dashed line), and 1.24 (green dash-dotted line), that all ensure 6 dB gain margins, assuming the use of critically damped accelerometers having their mounted natural frequencies of 42 kHz, 28 kHz, and 4.2 kHz, respectively, synthetizing the inertances of approximately 0.001 kg, 0.0035 kg, and 0.031 kg, respectively.

However, achieving the critical damping ratio in a miniature accelerometer system with a natural frequency of 42 kHz is not trivial. This is because the accelerometer critical damping coefficient, increases with its natural frequency, $c_{A,crit} = 2m_A\omega_A$. As an illustration, if the accelerometer inertial mass equals to $m_A = 0.001$ kg, then the required critical damping coefficient calculates to about 528 Ns/m. It is thus reasonable to consider an accelerometer with a lower natural frequency. Figure 5 shows that by reducing the natural frequency of the error accelerometers, it is possible to use higher feedback gains and to synthetize larger inertances. The critically damped accelerometer in fact behaves like a mechanical low-pass filter with a roll-off rate of 40 dB per decade above its natural frequency, Figure 4 (a), green dashed line. This is beneficial in terms of the feedback loop stability and the maximum admissible feedback gain, and thus, the maximum synthesizable inertance. However, the phase of the transfer function, H_S, is also altered by the filtering, and it lags by 90 degrees at the accelerometer resonance frequency. As a result, the Nyquist locus rotates clockwise in the real-imaginary plane indicating that the feedback loop produces a combination of relative acceleration and relative velocity feedback, Figure 4 (b). Therefore, by decreasing the natural frequency of the critically damped accelerometers, the antiresonances due to the synthetized inertances become characterised by increasing active damping effects and the vibration isolation objective may not be fully achieved.

4. CONCLUSIONS

An active control system emulating the effects of inerter element for vibration isolation is considered. It is in principle possible to apply direct relative acceleration feedback using inertial accelerometers and electrodynamic reactive actuators. For stability reasons it is necessary to use

highly damped accelerometers that effectively filter out the error signal above their natural frequency. In particular, by using critically damped accelerometers with a high natural frequency the desired inertance can be emulated by the control system. However, achieving large damping ratios in small-scale accelerometers with a high natural frequency is problematic. In accelerometers with a low natural frequency achieving high damping ratios is technically less challenging, but in such a case the natural frequency must not be too low in order to avoid the feedback loop delivering a combination of active inertia and active damping which compromises the vibration isolation effect.

ACKNOWLEDGEMENTS

This project has received funding from the European Union's Horizon 2020 research and innovation programme under the Marie Sklodowska-Curie grant agreement no. 657539.

REFERENCES

1. Schönfeld JC. Analogy of hydraulic, mechanical, acoustic and electric systems. Applied Scientific Research. [Online] Martinus Nijhoff, The Hague/Kluwer Academic Publishers; 1954;3(1): 417–450. Available from: doi:10.1007/BF02123920
2. Smith MC. Synthesis of mechanical networks: the inerter. IEEE Transactions on Automatic Control. [Online] 2002;47(10): 1648–1662. Available from: doi:10.1109/TAC.2002.803532
3. Renno JM, Mace BR. Vibration modelling of helical springs with non-uniform ends. Journal of Sound and Vibration. [Online] 2012;331(12): 2809–2823. Available from: doi:10.1016/j.jsv.2012.01.036
4. Smith MC, Wang F-C. Performance Benefits in Passive Vehicle Suspensions Employing Inerters. Vehicle System Dynamics. [Online] 2004;42(4): 235–257. Available from: doi:10.1080/00423110412331289871
5. Faraj R, Jankowski Ł, Graczykowski C, Holnicki-Szulc J. Can the inerter be a successful shock-absorber? The case of a ball-screw inerter with a variable thread lead. Journal of the Franklin Institute. [Online] 2019; Available from: doi:10.1016/j.jfranklin.2019.04.012
6. De Domenico D, Deastra P, Ricciardi G, Sims ND, Wagg DJ. Novel fluid inerter based tuned mass dampers for optimised structural control of base-isolated buildings. Journal of the Franklin Institute. [Online] 2018; Available from: doi:10.1016/j.jfranklin.2018.11.012
7. Brennan MJ, Garcia-Bonito J, Elliott SJ, David A, Pinnington RJ. Experimental investigation of different actuator technologies for active vibration control. Smart Materials and Structures. [Online] IOP Publishing; 1999;8(1): 145–153. Available from: doi:10.1088/0964-1726/8/1/016
8. Gonzalez-Buelga A, Clare LR, Neild SA, Jiang JZ, Inman DJ. An electromagnetic inerter-based vibration suppression device. Smart Materials and Structures. [Online] IOP Publishing; 2015;24(5): 055015. Available from: doi:10.1088/0964-1726/24/5/055015
9. Høgsberg J, Brodersen ML, Krenk S. Resonant passive-active vibration absorber with integrated force feedback control. Smart Materials and Structures. [Online] 2016;25(4): 047001. Available from: doi:10.1088/0964-1726/25/4/047001
10. Zhao G, Raze G, Paknejad A, Deraemaeker A, Kerschen G, Collette C. Active tuned inerter-damper for smart structures and its $\mathscr{H}\infty$ optimisation. Mechanical Systems and Signal Processing. [Online] Academic Press; 2019;129: 470–478. Available from: doi:10.1016/J.YMSSP.2019.04.044
11. Preumont A. Vibration Control of Active Structures. [Online] Cham: Springer International Publishing; 2018. Available from: doi:10.1007/978-3-319-72296-2
12. Balas MJ. Direct Velocity Feedback Control of Large Space Structures. Journal of Guidance, Control, and Dynamics. [Online] 1979;2(3): 252–253. Available from: doi:10.2514/3.55869
13. Alujević N, Tomac I, Gardonio P. Tuneable vibration absorber using acceleration and displacement feedback. Journal of Sound and Vibration. [Online] 2012;331(12): 2713–2728. Available from: doi:10.1016/j.jsv.2012.01.012
14. Alujević N, Čakmak D, Wolf H, Jokić M. Passive and active vibration isolation systems using inerter. Journal of Sound and Vibration. [Online] 2018;418: 163–183. Available from: doi:10.1016/j.jsv.2017.12.031
15. Rao SS. Mechanical vibrations. Prentice Hall; 2011. 1084 p.
16. Non-Comm DC Voice Coil Linear Actuator - NCC01-04-001-1X. [Online] Available from: https://www.h2wtech.com/product/voice-coil-actuators/NCC01-04-001-1X
17. Piezoelectric Charge Accelerometer Types 4371 and 4371-V. [Online] Available from: https://www.bksv.com/-/media/literature/Product-Data/bp2036.ashx